ADVANCED FUNCTIONAL MATERIALS
www.afm-journal.de

"Twin Chain" PVA Cryogels with Controlled Tortuosity as Advanced Materials for Cleaning of Works of Art

Rosangela Mastrangelo, Damiano Bandelli, Luciano Pensabene Buemi, and Piero Baglioni**

Soft matrices with tuned properties are part of the vast landscape of innovative materials for the restoration of works of art. "Twin chain" polymer networks (TC-PNs) based on polyvinyl alcohol have proven unique as scaffolds for Cultural Heritage cleaning. They enable optimum adaptability, adhesion, porosity, and connectivity at both micro- and nano-scale resulting in superior time/space-controlled cleaning operations. In this work, TC-PNs properties are tuned through a mild crosslinking of the poly(vinyl alcohol) (PVA)-porogen polymer by using sebacic, adipic, or succinic acid. The modified porogens have different structural features imparting a different phase behavior to TC-PVAs mixtures in aqueous solution, i.e., in pre-gel systems used to form gels through a liquid–liquid phase separation. The macro-, micro-, and nanoscale features of the final gels are characterized by Confocal Laser Scanning Microscopy, Small Angle X-ray Scattering, Rheology and are related to their cleaning performances. The study shows that the gels cleaning capacity is related to their tortuosity, that can be tailored at the nanoscale. Counterintuitively gels with higher tortuosity show better performances as evidenced by the cleaning of mockups and paintings from Jean Helion, Jackson Pollock, and Tancredi Parmeggiani at Peggy Guggenheim Collection in Venice.

1. Introduction

Nowadays, the development of protocols aimed at tuning material properties is a central feature to boost material's performance and safety for a vast range of applications such as biomedicine, engineering, agriculture, and cultural heritage preservation.[1–8] To this end, an in-depth knowledge of the physico-chemical phenomena affecting the materials final performances is mandatory to maximize their efficacy and safety for the desired application.[9–12] In the case of works of art exposed to dust, humidity and light, most of the degradative processes occur at the work of art surface, resulting in premature disfiguration, possibly leading to permanent deterioration.[13,14] In these cases, cleaning interventions are needed to restore the artwork's original appearance. Materials developed for the conservation of cultural heritage must provide optimal interfacial features, together with optimal tailored micro- and nanostructural properties to carry out their function. For example, porous matrix and scaffolds, developed for conservation purposes, must be able to embed cleaning fluids, allowing their diffusion at the interface and, at the same time, provide optimal interfacial features, such as roughness and adhesion, to grant a uniform cleaning action[15] on complex rough surfaces usually present on some of the most iconic paintings of Modern and Contemporary art (Pollock, Picasso, Twombly, Ernst, just to mention some).[14] Besides, the variety of artifacts' surfaces often require materials with different properties, making materials tunability a fundamental step to improve their versatility.[15]

Despite the apparent simplicity of this concept, the development of materials with superior performances requires remarkable attention to synthetic details, relying on specific micro- and nanostructural properties.

Nowadays, gels represent the most performing systems employed in cleaning practices, surpassing the "traditional" ones based on the direct use of solvent, solvent blends, or thickened solvents.[1,16–18] In fact, gels can greatly improve the removal of unwanted layers from a surface due to solvent entrapment and release control, adhesion, rheological properties, as well as macro- and microscopical features.[1,15] The choice of gelled materials to be employed in CH practices is often related to the nature of the layer to be removed from the painted surface. In principle, hydrophilic layers can be treated with hydrogels, i.e., networks able to upload water solutions and complex fluids, while organogels, i.e. networks able to upload organic solvents, could be employed for the removal of hydrophobic layers.[1,19] Most of the hydrogels currently developed and employed in CH practices are based on polymers such as polyacrylamide,[20] poly(2-hydroxyethylmethacrylate)

R. Mastrangelo, D. Bandelli, P. Baglioni
Department of Chemistry and CSGI
University of Florence
Via della Lastruccia 3, Sesto Fiorentino, Florence 50019, Italy
E-mail: damiano.bandelli@unifi.it; baglioni@csgi.unifi.it
L. Pensabene Buemi
Conservation Department
Peggy Guggenheim Collection
Dorsoduro 701, Venice 30123, Italy

The ORCID identification number(s) for the author(s) of this article can be found under https://doi.org/10.1002/adfm.202404287

DOI: 10.1002/adfm.202404287

(p(HEMA)), poly(vinylpyrrolidone) (PVP), and polyvinyl alcohol (PVA).[21,22] Polyacrylamide, p(HEMA) and PVP. These hydrogels present good compatibility but they feature low adaptability on rough surfaces. The recently developed PVA "twin chain" polymer networks (TC-PNs) represent the most interesting candidate due to the excellent resistance to mechanical stress and the enhanced adaptivity.[23–26] PVA TC-PNs are obtained via the freeze-thawing (FT) approach. In brief two PVAs, one with high degree of hydrolysis (HPVA) and another with lower degree of hydrolysis (LPVA) are dissolved in water. The mixture undergoes a spontaneous phase-separation: LPVA chains demix and concentrate in blobs, while HPVA is preferentially located in the continuous phase. The demixing is likely caused by the high molecular weight of both species, considering also the high propensity to self-interaction of HPVA chains[27] and the different hydration of the two phases,[23] which is known to lead to phase-separated systems for the production of macroporous gels.[28,29] Moreover, the presence of acetate groups on LPVA chains leads to collapsed or micelle-like conformations in aqueous solution[30] that can further facilitate the phase-separation. Once the phase-separated solution undergoes the freeze-thaw process, and the subsequent swelling in water, hydrogels with a sponge–like, interconnected porosity are obtained, as the porogen polymer is partially extracted during washing. These features enhance cleaning performances in CH practices.[23] More specifically, we found that the combination of specific polymer pairs influences the aqueous mixture phase-behavior, imparting to gels specific pores morphology at the micro-scale. Pores connectivity at the nanoscale can be tailored to obtain different gels apparent tortuosity. Tortuosity is related to solvent residence-time at the artwork-gel interface.[15] Counterintuitively, gel matrices with high tortuosity show the best cleaning performances: the higher the tortuosity, the higher the removal of unwanted layers from the work of art surface.

Recently, we have reported on the preparation of modified PVA TC-PN by employing a sebacic-acid crosslinked LPVA as porogen to control gel's porosity.[31] Overall, it has been shown how the use of a mildly crosslinked sebacic acid-LPVA porogen for PVA TC-PNs is favorable to tune i) the rheological properties of the gel, resulting in materials with higher adaptability to surfaces, ii) the micro- and nanostructural features, iii) the solvent compatibility, enabling the use of solvents with moderate hydrophobicity that are not compatible with PVA. The use of crosslinked sebacic acid-LPVA resulted in higher dirt removal on model surfaces as well as on real case studies.[31] In principle, further extension of the crosslinking density of the porogen species could be beneficial to improve further the gel's performance. This concept could result in the development of materials capable of removing an increased number of diverse types of soil, grimes, coatings and overpaints that represents recurrent and challenging restoration interventions.

To this purpose, we herein report the development of novel PVA TC-PNs, obtained employing LPVA crosslinked with adipic and succinic acid, and their comparison with the already established sebacic acid-functionalized porogen. The main features of the final porogens were assessed by means of size exclusion chromatography (SEC) equipped with multi-angle light scattering, viscosity and refractive index detectors to gain information on the crosslinked structure of the modified LPVA species. Then, the new porogenic additives were tested for the preparation of PVA TC-PNs and confocal laser scanning microscopy (CLSM) was employed to monitor the pre-gel phase separation and the gel's microstructure prior and after washing cycles in water. The gel's structural features, that proved a strict structure-property relationship, were investigated via small-angle X-ray scattering (SAXS), chord analysis, mechanical properties from rheological measurements, and tortuosity by fluorescence correlation spectroscopy (FCS) analysis. In view of their application in CH, cleaning tests were first performed on a model surface representative of typical modern/contemporary paint layers, followed by case studies selected from the Peggy Guggenheim Collection (Venice). The results highlight for the first time a clear relationship between the gels structure, tortuosity, and the cleaning performances, opening new perspectives in the fine tuning of structure-performances of this new class of gels.

Table 1. Detailed data from Size Exclusion Chromatography (SEC) equipped with MALS- Viscometer- RI detectors. If not noted otherwise, uncertainties are below the last decimals reported.

Code	M_n [a] [kg mol^{-1}]	Đ [b]	R_h [c] [nm]	α [d]	CS [e]
LPVA	154 ± 1	1.51 ± 0.01	10.0	0.68	0.58
LPVA-Seb	157 ± 1	1.88 ± 0.01	10.6	0.59	0.51
LPVA-Ad	170 ± 1	1.87 ± 0.01	11.3	0.50	0.42
LPVA-Suc	438 ± 6	1.80 ± 0.01	15.4	0.47	0.39

[a] Number average molar mass (M_n) obtained via SEC-MALS analysis in the DMSO/DMF eluent; [b] Molar mass dispersity index (Đ) obtained via SEC-MALS analysis in the DMSO/DMF eluent; [c] Hydrodynamic radius (R_h) obtained via SEC-MALS analysis in the DMSO/DMF eluent; [d] Parameter α of Mark-Houwink obtained as slope of the log-log plot of intrinsic viscosity over molar mass from data collected with SEC analysis; [e] Conformational slope (CS) obtained as slope of the log-log plot of the radius of gyration (R_g) over molar mass from data collected with SEC analysis.

2. Results and Discussion

The scope of the present work is based upon the development of new crosslinked polymeric additives to be employed for the preparation of TC-PNs of PVA. To this aim, a literature protocol was employed for the functionalization of poly(vinyl alcohol-*co*-vinyl acetate) (POVAL 32–80) with sebacic, adipic and succinic acid.[31] Briefly, the functionalization was performed in bulk for 1 h at 120 °C employing a 2.5 mol.% feed of the selected acid over the PVA's hydroxyl groups. The final products were characterized by means of size exclusion chromatography (SEC) equipped with multi angle light scattering (MALS)-Viscometer-refractive index (RI) detectors to gain information on the molar mass and the structural features of the modified PVAs (**Table 1**).[32,33]

As expected from previous data,[31] the functionalization resulted in a slight increase of the number average molar mass (M_n) from 154 kg mol^{-1} of the unmodified sample LPVA to 157 and 170 kg mol^{-1} after functionalization with sebacic and adipic acid, respectively (LPVA-Seb and LPVA-Ad) due to the ability of dicarboxylic acids to crosslink LPVA chains. In contrast, almost a triplication of M_n of 438 kg mol^{-1} was calculated for the LPVA-Suc sample revealing that adipic acid was more prone to react with LPVA resulting in higher degree of crosslinking. At the same time, the functionalization affected the dispersity index that raised from 1.51 of LPVA to values of 1.80 to 1.88 for

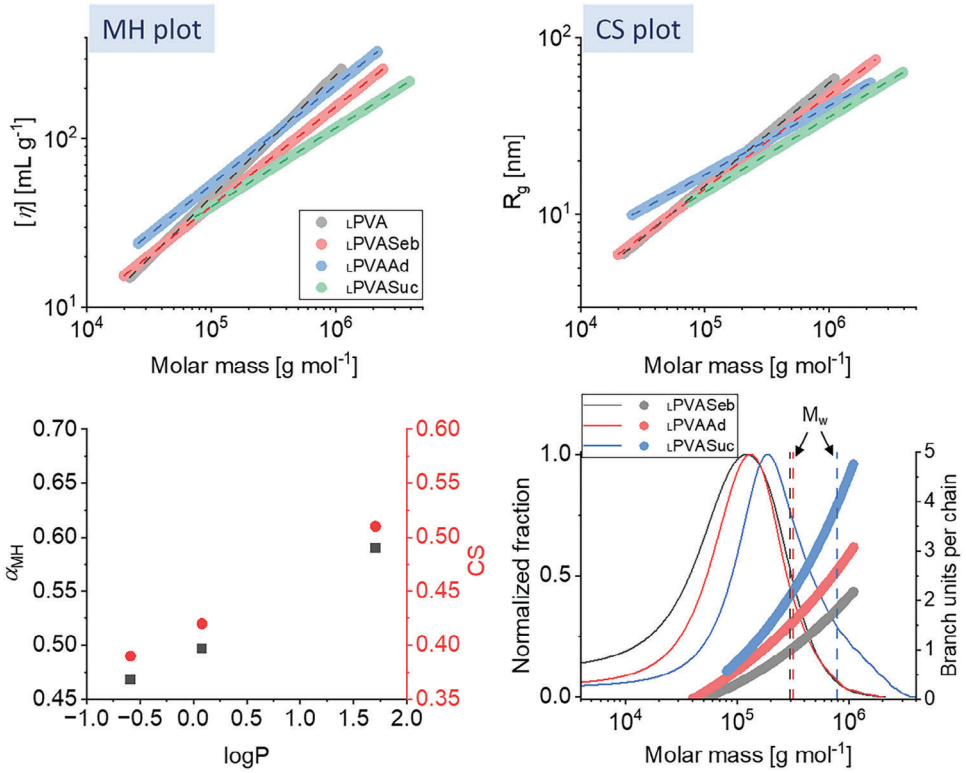

Figure 1. Size Exclusion Chromatography (SEC) analysis of the PVA library. **Top left**. Log-log plot of the intrinsic viscosity, [η], over molar mass (dots) and linear fitting according to the Mark-Houwink (MH) equation (lines). The α parameters were extracted as the slope of the linear fitting. **Top right**. Log-log plot of the radius of gyration (R_g) over molar mass (dots) and linear fitting (lines). Conformational slopes (CS) were extracted as the slope of the linear fit. **Bottom left**. Evolution of the parameter a of MH (black dots) and the conformational slope (CS, red dots) over the dicarboxylic acid logP, i.e., the logarithm of the water/octanol partition coefficient. **Bottom right**. Evolution of the normalized weight fraction of polymer and the branch units per chain (U) over molar mass for the PVAs after reaction with sebacic, adipic and succinic acid. The vertical dotted lines represent the PVA's weight average molar mass (M_w).

the samples obtained after reaction. Overall, the effect of functionalization resulted in the variation of the hydrodynamic radius, $R_{h,}$ calculated from SEC-viscometric analysis, that increased from number-average values of 10 nm for LPVA up to 15.4 nm for LPVA-Suc. Therefore, the reaction with dicarboxylic acid resulted in an increase of the polymer's hydrodynamic volume. In principle, the R_h increase could be ascribed to a more extended polymer conformation in solution, typically found for functionalized polymers, or could be related to crosslinking. To evaluate the causes of R_h increase, additional information were obtained by fitting the log-log plot of the intrinsic viscosity ([η], i.e., the viscosity of a solution ideally containing one macromolecule) over molar mass according to the Mark–Houwink (MH) equation which enabled calculating the parameter α, related to conformational changes in solution (**Figure 1** and Equation (3)).

$$[\eta] = k \cdot M^{\alpha} \quad (1)$$

where M is the molar mass of the polymer, while k and α are the Mark–Houwink parameters describing polymer–solvent interactions, and thus giving insights on the functionalization/crosslinks.

In detail, the α parameter in the range between 0.78 to 0.50 indicates good solvent regime, α = 0.50 is the theta condition, and values below 0.50 are indicative of poor solvent regime. As a result, the unfunctionalized LPVA featured an α of 0.68, within the good solvent regime. Upon reaction with sebacic acid, α decreased to values of 0.59 still suggesting good polymer-solvent interactions in line with literature data.[31] The reaction with adipic acid resulted in an α value of 0.50 that represent the theta condition, while the reaction with succinic acid resulted in a value of 0.47 suggesting a denser packing of the polymeric chains due to crosslinking.

Additionally, the log-log plot of the radius of gyration and the molar mass (Figure 1) were fitted with linear regressions to calculate the conformational slopes (CS). As a result, a CS of 0.58 was calculated for LPVA, while functionalization resulted in the CS trend as following: LPVA-Seb (0.51) > LPVA-Ad (0.42) > LPVA-Suc (0.39), in line with the MH evaluation. Overall, both the α parameter of MH and the CS suggested that the reaction of succinic acid with LPVA, produced the strongest variation of the polymer morphology in solution for the Seb, Ad and Suc derivatives. The evaluation of molar mass, α and CS values obtained from SEC analysis revealed that the functionalized LPVA featured a more packed structure in comparison with the unfunctionalized LPVA. As a result, the R_h increase could be ascribed to the effect of crosslinking between LPVA polymer chains promoted by the reaction with dicarboxylic acids.

Considering that dicarboxylic acids differ in the spacer length between the carboxyl moieties, we hypothesized that the different molar mass increase and the different solution behavior (from α and CS) were related to the different compatibilization between polymer and crosslinker, due to hydrophilic/hydrophobic interactions. An estimation of such behavior was obtained employing the plot of a and CS over logP, i.e., the logarithm of the water/octanol partition coefficient, of the dicarboxylic acids (Figure 1). As a result, a seemingly linear trend was obtained suggesting that the increase of the carboxylic acid hydrophilicity increases their reactivity toward PVA.

To evaluate the crosslinking efficiency of the process, the number of branch units per chain (U) was calculated on the basis of SEC data employing the viscosity method expressed in Equation (2) that we have recently applied for similar PVA chains crosslinked with sebacic acid.[31,32,34]

$$\left(\frac{[\eta]_{Crosslinked}}{[\eta]_{Linear}}\right)^{e} = \left[\left(1+\frac{U}{7}\right)^{1/2} + \frac{4U}{9\pi}\right]^{-1/2} \quad (2)$$

where $[\eta]_{Crosslinked}$ is the intrinsic viscosity of the crosslinked sample, $[\eta]_{Linear}$ is the intrinsic viscosity of the linear polymer, e is the draining parameter that was assumed equal to 0.75 for all the samples according to recent literature.[35]

The evaluation of the U parameter is summarized in Figure 1 (bottom right) and depicts a U trend that follows the order LPVA-Suc > LPVA-Ad > LPVA-Seb, as expected from both MH and CS plots. Therefore, the number of branch units per chain extrapolated at the weight average molar mass (M_w) followed the same trend LPVA-Suc (3.9) > LPVA-Ad (1.5) > LPVA-Seb (1.0).

This indicates that crosslinking efficiency was maximized when the dicarboxylic acid's spacer length and its logP were minimized.

Overall, the reaction of LPVA with sebacic, adipic and succinic acid enabled the variation of hydrodynamic radius (R_h) and structural features (M_n, α and CS), making the final polymeric samples ideal candidates for the preparation of TC-PN prepared via freeze-thawing (FT) of PVA semi-diluted solutions.

To this aim, pre-gel solutions were obtained by mixing HPVA and one of the functionalized LPVA (LPVA-Seb, LPVA-Ad or LPVA-Suc) in a 3:1 mass ratio. The morphology of the systems prior to FT was investigated through CLSM: **Figure 2** shows a micro-phase separation occurring in all pre-gel solutions ("Sol" row in the figure). More specifically, the green areas, i.e., the continuous phase, preferentially contains HPVA (covalently labeled with FITC), while the porogens (non-labeled) are mainly localized in blobs. Blobs size decreases along the LPVA-Suc > LPVA-Ad > LPVA-Seb series, i.e., increasing the dicarboxylic acid's logP. Overall, the decrease of blob size follows the trend depicted for the crosslinking units per chain and suggested that phase separation follows the LPVA ability to interact with the surrounding media.

Afterward, PVA TC-PNs were obtained via freeze-thawing. TC-PNs were named, according to the nomenclature given to the crosslinked LPVA porogens, as PVA-Seb, PVA-Ad and PVA-Suc. The freeze-thaw process leading to systems gelation alters the samples morphology: while blobs act as porogens for the final gels, HPVA form the networks main structure (FT gel in Figure 2). It is worth noting that HPVA strands run also through the blobs, likely forming channels, and leading to the hierarchical, interconnected porosity that grants TC-PNs excellent transport properties.[27,36,37]

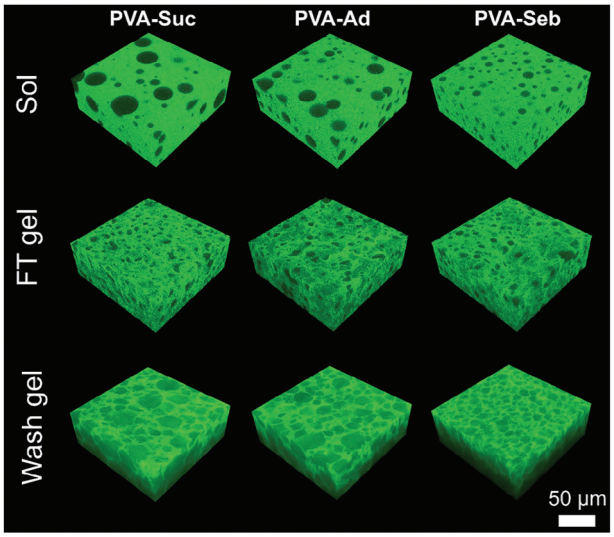

Figure 2. Confocal 3D images of pre-gel solutions, freeze-thawed (FT) and washed gels.

Washed gels (Wash gel row in Figure 2) show large pores in the micron-scale, whose size can be related to the blobs size present in pre-gel solutions. More specifically, pores are lager in PVA-Suc gel, and decrease in PVA-Ad and PVA-Seb. Average pores size was obtained through the chord analysis distribution method.[38,39]

In this regard, a set of 2D images was extracted from 3D stack of each gel and a set of randomly oriented lines was drawn on each of them. Each time a line crosses phase boundaries, a segment is extracted. Segments (i.e., chords) are finally collected, depending on their length and frequency of occurrence, as shown in **Figure 3A**. Chords distributions show a peak and an exponential tail. The characteristic pores length, λ, of each system was extracted from the latter. λ values are reported in **Table 2**.

Moreover, all data show a small plateau between 5 and 10 μm (see arrow in Figure 3A), indicating a typical pore dimension shared by all networks.

The characteristic pore size confirms that a clear trend can be traced: pores dimension increases as the carbon chain of the fatty acid becomes shorter. More specifically, λ ranges between 5 and 7 μm, while pores distribution is significantly wider in PVA-Suc (see the intercept with x-axis in Figure 3). In other words, pores are larger but also more polydisperse in PVA-Suc network. The use of different fatty acids to modulate the porosity was more effective in increasing the gels pore size than using the same fatty acid on L-PVAs of different M_w or hydrolysis degree as reported in previous studies.[31]

We recently found that gels morphology at the micron-scale can be related, to some extent, to pores size and connectivity at lower dimensions.[15] More specifically, gels with modulated porosity at the micron-scale may exhibit different tortuosity at the nanoscale, which can be related, in turn, to gels cleaning abilities. To elucidate pores connectivity at the nanoscale, we measured the gels apparent tortuosity through FCS. Using a recently validated

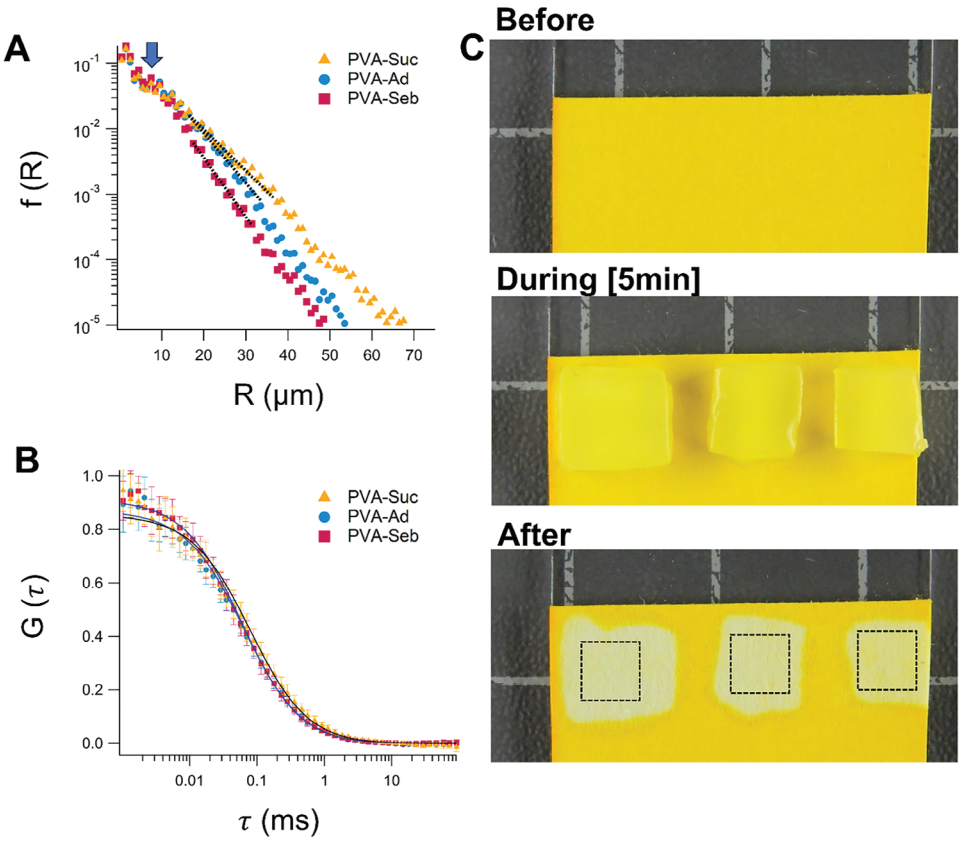

Figure 3. A) Chord length distribution of gels pores; B) FCS curves and fitting to calculate the diffusion coefficient of Alexa Fluor in gels, after the interaction with a dyed cardboard support; C) Gels cleaning ability toward water-soluble molecules, i.e., ability to extract tartrazine from a cardboard support after a 10 minutes interaction.

protocol,[15,27] we measured the diffusion of the dye Alexa Fluor 568, commonly used for FCS calibration, within the networks and after the interaction of gels with a tartrazine-dyed cardboard (10 minutes). FCS curves and fitting are shown in Figure 3B, while the extracted diffusion coefficients, D_{Gel}, and the apparent tortuosity, calculated as $\tau^2_{app} = D_{Sol} / D_{Gel}$ (see Experimental section) are listed in Table 2. Gels apparent tortuosity increases with the average pore size at the micron-scale, being PVA-Suc the gel characterized by the most irregular flow paths. Tortuosity decreases as PVA-Suc > PVA-Ad > PVA-Seb.

As hPVA strands characterize the whole gel matrix during the freezing process (see FT gel row in Figure 2), it is likely that larger phase-separated domains favor the formation of a hierarchical porosity with a wider pore size distribution at all length scales.

As previously mentioned, tortuosity can be related to gels cleaning abilities. We tested gels removal capability on the same tartrazine-dyed carboard used for FCS experiments. Tartrazine is a water-soluble dye, that neither interacts with PVA, nor with Alexa Fluor.[40] Therefore, tartrazine removal from the support can be related to the gels capture of the tartrazine water-soluble molecules.

Cleaning tests on tartrazine-dyed carboards are shown in Figure 3C, while cleaning efficacy can be inferred by the average, maximum and minimum greyscale values calculated in cleaned areas (Table 2). Briefly, greyscale intensity of pixels in the image ranges from 0 (black) to 255 (white). Therefore, the greyscale intensity values indicate that PVA-Suc is the most effective system for the removal of hydrosoluble compounds. This result can be

Table 2. Slope, 1/ λ, extracted from f(R) vs. R graph, gels characteristic pores length, λ, diffusion coefficient of Alexa Fluor 568 in gels, D, gels apparent tortuosity, τ_{app}^2. Average, minimum and maximum intensity of pixels calculated in the cleaned areas of the dyed cardboard (squares of 4 × 4 mm^2, greyscale image; black = 0, white = 255).

Gel	1/λ (Pores)	λ [Pores, μm]	D [μm^2/s]	τ^2_{app}	Average greyscale intensity	Min intensity	Max intensity
PVA-Suc	0.15 ± 0.01	6.9	113 ± 7	2.5	196 ± 4	177	220
PVA-Ad	0.18 ± 0.01	5.7	142 ± 7	2.0	193 ± 4	165	217
PVA-Seb	0.21 ± 0.01	4.8	151 ± 8	1.8	187 ± 4	151	213

The diffusion coefficient of free Alexa Fluor in a tartrazine aqueous solution is D_{Sol} = 278 ± 14 μm^2/s.[27]

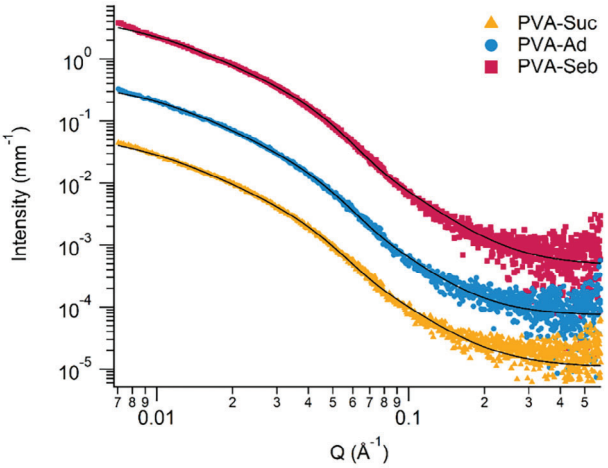

Figure 4. SAXS curves (markers) and fitting (black solid lines) of gels.

related to the system apparent tortuosity, leading to an important evidence: a higher tortuosity implies longer residence times of the cleaning solution at the gel-carboard interface,[15,27] resulting in a higher local removal before the fluid diffuses through the gel matrix.

Additional details on gels nanoscale features were obtained through SAXS measurements. SAXS curves and fitting, performed according to Equation (7) (see Experimental Section), are shown in **Figure 4**. Fitting parameters are listed in **Table 3**.

Gels features at the nanoscale show slight variations among the samples. The correlation length ξ, indicating a mesh-size in liquid-like gel portions, is slightly larger in PVA-Suc gel. The fractal dimension D and the PVA crystallites radius, R, are almost constant along the series. The I_G/I_L ratio, indicating the prevalence of solid-like (crystalline) areas over liquid-like gel portions, is slighly higher in PVA-Suc sample, suggesting a higher local structuration in this sample.

Nonetheless, it is worth noting that this gels shows ξ values generally higher than those of gels belonging to the TC-PNs class,[23,27,37] and comparable to networks obtained through the decoration of the porogen chains with fatty acids.[31]

The mechanical properties of decorated TC-PN gels with tuned nano- and microstructure were analyzed by rheometry. For all the TC-PNs, amplitude sweep analysis revealed a similar storage modulus (G') and loss modulus (G'') in the range between 5 and 0.01 oscillation strain %, proving the conservation of the mechanical properties when moderate forces were employed. Given the linear response of G' and G'' to the oscillation strain experiments, frequency sweeps experiments were performed with an oscillation strain of 1% (**Figure 5**).

Frequency sweeps analysis revealed that both the storage and loss moduli, G' and G'', decreased in the order PVA-Suc > PVA-Ad > PVA-Seb. This result suggests that the use of additives for PVA TC-PN with higher degree of crosslinking, i.e., with lower spacer length between crosslinked chains, enables the tuning of mechanical properties by acting on the gel's microstructural features such as pore and wall size. Moreover, a simple comparison between G' (or G'') with the carboxylic acid's logP suggested a linear correlation between the hydrophilic/hydrophobic features of the starting reactants with respect to the final material properties, hinting to a strict relationship between the reactant choice and the final material properties. Overall, the TC-PNs herein reported feature lower G' and G'' moduli in comparison with gels reported in literature for cultural heritage conservation.[21,22,41–43] In principle, the reduction of the material's G' values enables the maximization of surface adaptivity since it favors the adhesion of the gels to rough surfaces. However, also microstructural features such as the presence of interconnected pore size in the gel network play a central role for the removal of dirt from surfaces, i.e., one of the key steps in cultural heritage preservation. In fact, an optimum interconnected porosity could enhance soil/dirt removal during cleaning applications due to surface capture and diffusing/retaining mechanisms.

The comparison of microstructural and mechanical features revealed that the PVA-Seb sample featured the lowest pore size and the highest adaptivity (lowest G' value), while PVA-Suc sample had the highest pore size and lowest adaptivity among the three gelled systems. Since the balance of the two abovementioned features plays a central role in remedial practices of CH preservation, applications on mockups representative of modern/contemporary painted surfaces were performed.

To this aim, the gelled systems were tested on a cadmium red alkyd mockup, representative of modern/contemporary paintings. Prior to the cleaning procedures, the PVA TC-PN gels were sampled in sheets with a dimension of ≈2.0×2.0×0.2 cm^3 and were immersed in a water solution containing triammonium citrate (TAC, 5 wt%) overnight, to enable the uptake of TAC in the gels interconnected porosity. Afterward, gels were gently blotted on paper to remove water excess and, finally, were applied on the surface for 3 minutes, without applying any mechanical stress.

The results of the cleaning indicate that the PVA-Suc gel had the highest performance, while PVA-Seb showed the poorest results (**Figure 6**). This indicates that the balance of micro- and macrostructural features plays a major role in the gel's capability of soil removal. On one hand, a high storage modulus is related to a reduced adaptability to the surface, that could, in principle, be a disadvantage, since it decreases the area of the gel interacting with the surface. On the other hand, tortuosity represents a key feature to vary the diffusion of cleaning solvents and their release

Table 3. SAXS fitting parameters of the investigated gels.

Sample	Guinier Scale $I_G(0)$	Lorentz Scale $I_L(0)$	$I_G(0)/I_L(0)$ ($\times10^{-2}$)	Correlation Length ξ [nm]	Fractal Dimension (D)	Crystallites Radius R [nm]	Background (Bkg), ± 0.0001
PVA-Succ	0.248	3.91	6.3	8.2 ± 0.1	2.9 ± 0.1	5.5 ± 0.1	0.0007
PVA-Ad	0.227	3.86	5.9	7.2 ± 0.1	3.1 ± 0.1	5.3 ± 0.1	0.0007
PVA-Seb	0.334	4.73	7.1	7.8 ± 0.1	3.0 ± 0.1	5.2 ± 0.1	0.0005

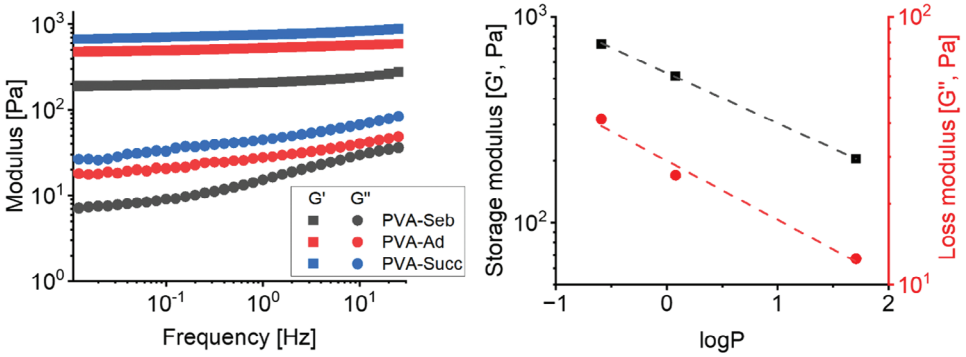

Figure 5. Frequency sweep analysis of PVA-Seb, PVA-Ad and PVA-Suc. **Left**. Evolution of the storage (square dots) and loss (circular dots) moduli over frequency. **Right**. Plot of the storage and loss modulus over the dicarboxylic acid logP for data extracted at 0.5 Hz (dots) along with their trend (dotted lines).

from the gel. PVA-Suc, i.e., the most active candidate for soil removal, featured the lowest adaptability of the TC-PN series, while it featured the highest tortuosity. In contrast, PVA-Seb, featuring the lowest soil removal performance, had the highest adaptability and the lowest tortuosity while PVA-Ad, with average performance had also average properties. Overall, data collected suggest the central importance of tortuosity, related to the capability of solvent mixtures/fluids to diffuse in the gel matrix and at the interface.

To prove the efficacy of the method proposed for the development of hydrogels with superior performances in CH practices, the PVA TC-PNs were tested on real case studies from the Peggy Guggenheim Collection (Venice). To this aim, the three PVA TC-PN gelled systems were immersed in an aqueous solution containing triammonium citrate (TAC, 5 wt.%) overnight, as described before for the gel's applications on the model mockup.

Cleaning tests were performed on "Equilibrium" from Jean Hélion (1933-1934), Untitled (Composition) from Tancredi Parmeggiani (1955) and on "Croaking Movement" from Jackson Pollock (1946) belonging to the Peggy Guggenheim collection (Venice) (**Figure** 7). Both paintings were affected from soil/dust adsorption during the last decades, resulting on surface's discoloration. In this case, the direct use of cleaning fluids on the surface is discouraged, due to paint sensitivity, possibly leading to pigments leaching. For this reason, the use of gelled systems capable of tuning solvent dynamics is of outmost importance to

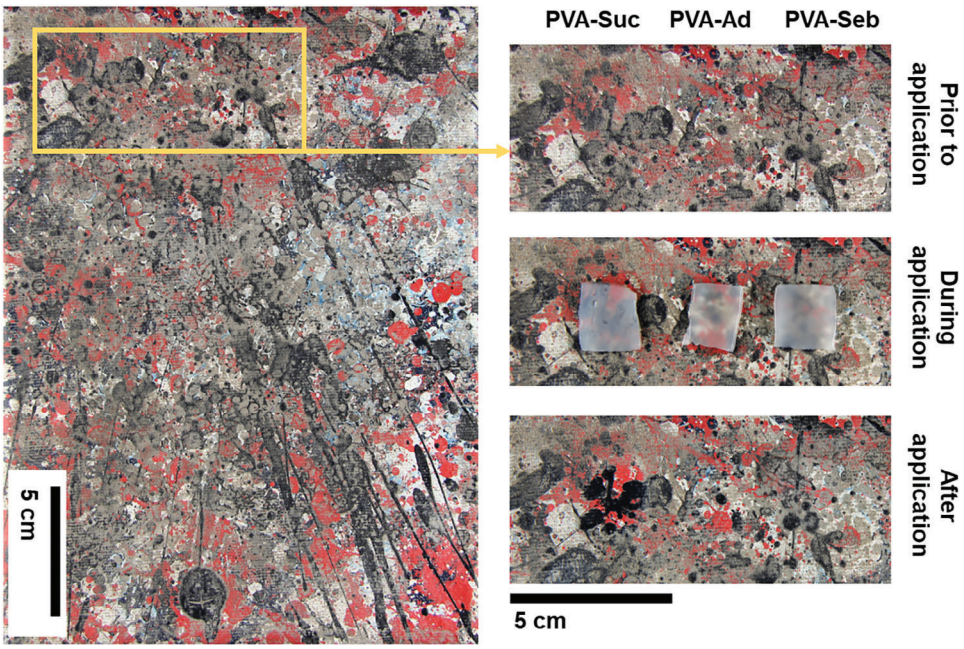

Figure 6. Application of the PVA TC-PN gelled systems on an artificially soiled alkyd mockup with increased surface roughness, representative of typical paint layers found in modern/contemporary art. **Left**: Image of the overall sample, the rectangle area boxed in yellow was chosen for the application of the PVA TC-PN gelled systems after equilibration with TAC (5 wt.%). **Top right**: Zoom-in in the region of gel's application prior to the cleaning procedure. **Middle right**: Zoom-in in the region of gel's application during the cleaning procedure. **Bottom right**: Zoom-in in the region of gel's application after cleaning.

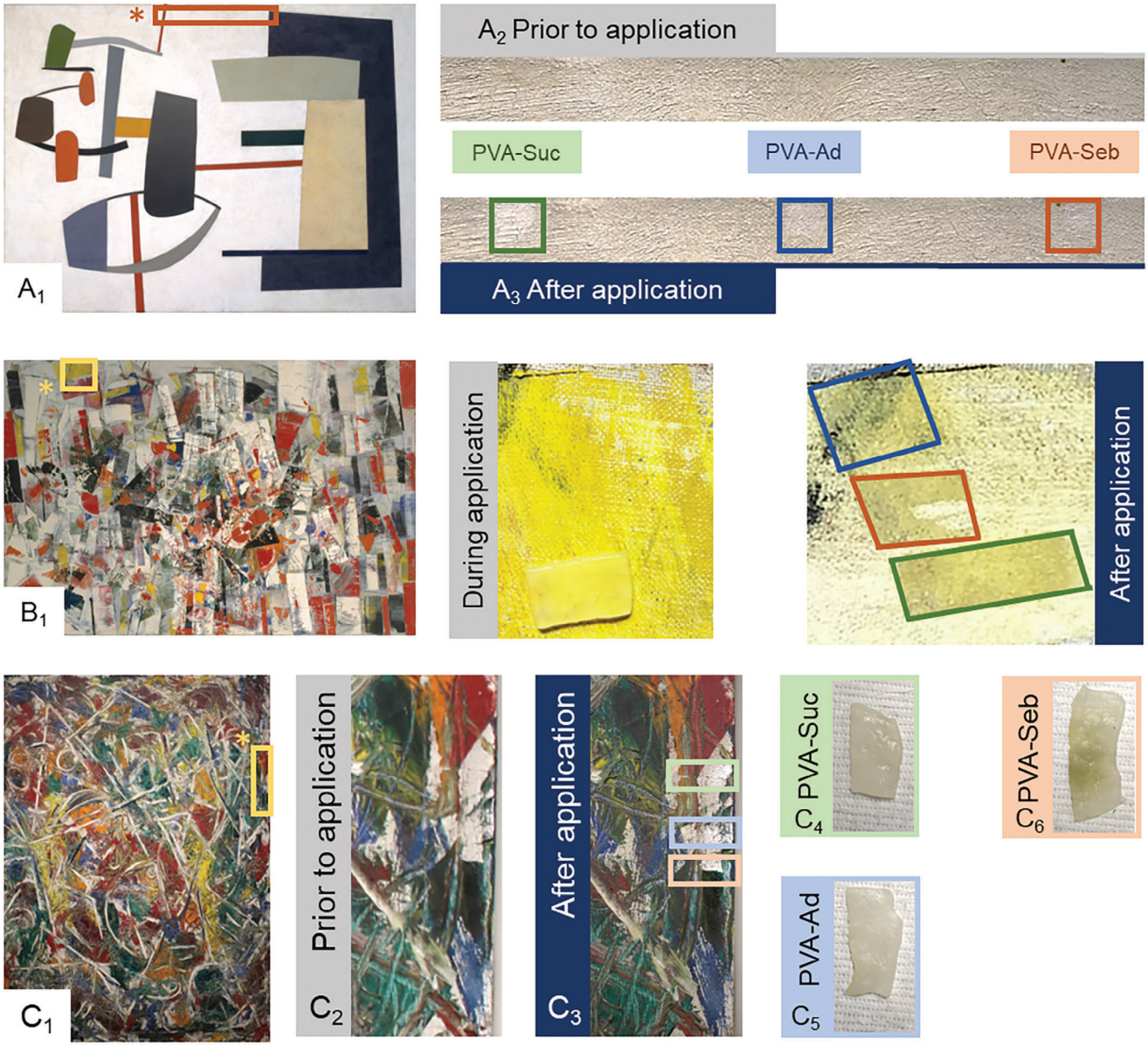

Figure 7. The three canvas paintings belonging to the Peggy Guggenheim Collection (Venice) cleaned using the PVA TC-PNs. A) **Top row**. A_1) "Equilibrium" from Jean Hélion (1933-1934). The rectangular area boxed in orange was treated with the PVA TC-PNs. Details of A_2) the painting area prior to gel application and A_3) after gel applications. B) Mid row. B_1) Untitled (Composition) from Tancredi Parmeggiani (1955). The rectangular area boxed in yellow was treated with the PVA TC-PNs. Details of B_2) the painting area during gel application and B_3) after gel applications. C) **Bottom row**. C_1) "Croaking Movement" from Jackson Pollock (1946). The rectangular area boxed in yellow was treated with the PVA TC-PNs. C_2) Details of the painting area prior to gel application and C_3) after gel applications. C_4 to C_6 the PVA TC-PNs gels after applications.

obtain the desirable cleaning efficacy without altering the painting's surface.

Applications on "Equilibrium" from Jean Hélion were performed to investigate the cleaning capability of the PVA TC-PNs on a soiled white area (Figure 7A). In fact, white discoloration is one of the most typical forms of soil and/or degradative contamination affecting surface appearances in unvarnished modern artifact. Overall, the application of the gelled PVA networks was carried out for 3 minutes and resulted in an excellent soil removal for PVA-Suc, followed by PVA-Ad and PVA-Seb (Figure 7A_3). Overall, the data confirmed the results of the preliminary tests on soiled alkyd-painted mockup (Figure 6) proving the effectiveness of the synthetic design of the PVA TC-PNs. Aiming at further extending the field of applications of the PVA TC-PNs, "Untitled (Composition)" from Tancredi Parmeggiani (1955) was also treated with the gels to further prove the gels cleaning performance. Cleaning tests resulted on the removal of soil deposited on the painting surface and featured the same trend of performances observed for "Equilibrium" from Jean Hélion.

Finally, the gels were employed for the cleaning of "Croaking Movement" from Jackson Pollock. This masterpiece features a thick, multicolored complex texture given by the artist's

painting technique (Figure 7B$_3$). Independently on the gelled system tested, gels application enabled the removal of dust layers, and resulted in the recovering of the original pigments, confirming the same cleaning efficacy trend: PVA-Suc > PVA-Ad > PVA-Seb.

Such safe and effective cleaning of complex surfaces can drastically decrease the application time, avoiding possible swelling of the pictorial layer as it might occur when traditional methodologies, mostly based on the use of free solvents or polymer-thickened solvents, are employed.

The reaction of sebacic, adipic or succinic acid with LPVA enabled the preparation of a new class of PVA with tunable degree of crosslinking and hydrodynamic radius as demonstrated from SEC analysis. As a result, the use of the newly established LPVA series for the preparation of PVA "twin chain" polymer networks enabled the controlled variation of the gel's micro and macro features. In particular, the use of LPVA-Suc, i.e., the LPVA with the highest degree of crosslinking, determined the formation of larger gel's pores at the microscale, higher tortuosity, and higher gel's stiffness, i.e., lower surface adaptivity, as detected from CLSM, FCS and mechanical (rheology) analysis. Decreasing the degree of crosslinking in the LPVA series resulted in smaller pores, lower tortuosity, and lower stiffness. It is expected that the cleaning performances of gelled systems are strongly related to an increased gels adaptivity.[1,15,31] Conterintuitively, the cleaning procedures of model surfaces mimicking modern/contemporary paintings affected by soiling, revealed the opposite trend. The same results were obtained when the gels were tested on masterpieces by Jean Hélion (Equilibrium, 1933–1934), Tancredi Parmeggiani (Untitled (Composition), 1955) and Jackson Pollock (croaking movement, 1946) belonging to the Peggy Guggenheim collection (Venice).

The cleaning results from model and real case studies suggested the presence of an additional driving force affecting cleaning performances. In this regard, also the gel's ability to transport cleaning fluid at the surface of a work of art is of paramount importance to boost the cleaning capability. This feature can be accessed at the nanoscale, by monitoring the tortuosity that gives a direct estimation of the molecular diffusion inside the gel's interconnected porosity nearby the surface region. Adaptivity and transport properties of gelled systems used in cultural heritage practices are often in accordance, and do not enable the decoupling of the effect related to a single feature.[15,23,31,36]

However, since the protocol of gel preparation introduced in this work enabled the complete decoupling of stiffness-tortuosity relationship, the higher performances of PVA-Suc gel could be associated with the gel's transport features. Interestingly, better cleaning results were obtained when the cleaning fluids diffusion is reduced at the boundary surface between substrate and gel, i.e., when gel tortuosity is higher.

Overall, we attributed the increased capability of PVA-Suc gel to the gel's capacity of slowing down molecular motions at the boundary surface between substrate and gel.

We believe that this new finding will be valuable for the design of materials with enhanced performances at the surface of objects, also beyond Cultural Heritage preservation scopes and aim.

3. Conclusion

In the last decades, the development of materials capable of performing complex functions on target surfaces has been a central topic in material science. To this aim, a multitude of parameters should be tailored to obtain high performances. For instance, materials for the restoration of paintings and canvas, that are among the most iconic objects in CH practices, should be capable of removing discolored layers produced by dust and degradative processes. The use of gelled materials has been proven to be a great advancement over traditional approaches, based upon an uncontrolled release to the work of art of solvents or solvent mixtures. In this regard, the recently developed PVA "twin-chain hydrogels"[23] represent the most performing systems for the cleaning of modern and contemporary artifacts as assessed on paintings by Pablo Picasso, Jackson Pollock, Gastone Novelli.[23,31]

The twin-chain polymer networks (TC-PNs), obtained from the mixture of two PVA samples with different hydrolysis degree and molar mass, benefit from the liquid-liquid phase separation during the gels cryo-formation, resulting in materials with sponge-like interconnected porosity, optimal for solvent transport. Recently, we have demonstrated the use of mildly functionalized PVA porogens with sebacic acid to produce TC-PNs with increased performances in CH everyday practices due to the refinement of micro-, nano-structure, and rheological properties with regards to the use of linear PVA chains as porogens.

In the present work we do not only expand the concept of functionalizing porogenic species via the use of alternative crosslinkers (adipic and succinic acid), but we introduce the central importance of tortuosity as a tool to control the gel's performances.

The structural evaluation of the porogens (LPVA) functionalized with adipic and succinic acid as crosslinkers was compared with the sebacic acid-decorated LPVA. The results showed an increased reactivity of succinic acid, resulting in higher degree of crosslinking, followed by adipic and sebacic acid. The crosslinked LPVA porogens were used along with fully hydrolyzed PVA, HPVA, in synthetic processes to synthesize TC-PNs gels derivatives. As a result, all the PVA cryogels exhibit a disordered, interconnected sponge-like porosity. In addition, the functionalization with succinic acid, in the PVA-Suc, produced bigger pores at the microscale, while adipic and sebacic acid-functionalized PVAs featured smaller ones, keeping similar nanostructural features. At the same time, tortuosity decreased in a similar fashion with the trend of PVA-Suc > PVA-Ad > PVA-Seb. Conversely, rheological properties had the opposite trend, suggesting higher adaptivity for the sebacic acid-functionalized TC-PNs gels.

Gels application to remove soil from mockup surfaces showed that the best performance of PVA-Suc TC-PN correlates the tortuosity parameter with the highest soil removal, followed by PVA-Ad and PVA-Seb.

Finally, the gels were tested for the cleaning of real case studies from the Peggy Guggenheim collection (Venice) to validate the initial screening. In the first instance, cleaning tests on "Equilibrium" from Jean Hélion (1933-1934) and on Tancredi Parmeggiani (Untitled (Composition), 1955) were performed to remove soil layers enabling the restoration of the original canvas background. The results validated the PVA-Suc > PVA-Ad > PVA-Seb cleaning trend. Moreover, when PVA-Suc was employed, a

complete soil removal was obtained in a fast (3 minutes) and controlled manner on the Hélion's white painting background. This represents a clear improvement of restoration practices over traditional methods requiring numerous time-consuming cleaning steps to avoid swelling and pigments leaching from the original painted layers. The cleaning capability on rough/complex surfaces was further tested on "Croaking Movement" from Jackson Pollock (1946) and "Untitled (composition)" (1955) from Tancredi Parmeggiani resulting in the same cleaning trend.

Overall, the use of succinic acid as a crosslinker for the preparation of new porogens for PVA TC-PNs proved to be optimal at improving TC cryogels cleaning capacity for the restoration of artifacts. Moreover, the comparison with PVA TC-PN cryogels obtained from three different porogens (adipic, sebacic and succinic acid) was pivotal for the evaluation of how tortuosity and its balance with the material's stiffness could affect the boundary layer between the gel and the treated surface. Given the feasibility and versatility of the preparation of this class of TC-PNs, the new functionalized PVA cryogels are ideal candidate also in transversal fields to Cultural Heritage conservation, such as biomedicine and tissue engineering, where surface diffusive phenomena are fundamental for regulating molecular transport.

4. Experimental Section

Materials: Poly(vinyl alcohol) with high degree of hydrolysis (99%, HPVA) and high molecular weight (160 kDa) was purchased from Sigma Aldrich. Poly(vinyl alcohol-*co*-vinyl acetate) with an hydrolysis degree 80% (LPVA) was kindly supplied by Kuraray (POVAL, 32–80). Sebacic acid (98%), adipic acid (>99%), and succinic acid (>99%) were purchased by TCI chemicals. Triammonium citrate (>97%, TAC) was purchased from Sigma–Aldrich.

The following fluorescent dyes were used for Confocal Laser Scanning Microscopy (CLSM) measurements: Fluorescein isothiocyanate isomer I (purity ≥ 90%, FITC, Sigma-Aldrich); Rhodamine 110 chloride (purity ≥ 99%, Sigma-Aldrich); Alexa Fluor 568 (Thermo Fisher Scientific). Tartrazine (Dye content ≥85%, Sigma–Aldrich) was used in the Fluorescence Correlation Spectroscopy (FCS) and cleaning test experiments. Ultrapure water was obtained by a Millipore MilliRO-6 Milli-Q gradient system (resistivity >18 MΩ cm). All chemicals were used without any further purification.

Functionalization of LPVA: A water solution containing LPVA (10 m/v%, 10.0 g) was prepared in pure water and mixed with sebacic, adipic or succinic acid to gain a dicarboxyl acid to hydroxyl molar ratio of 2.5 mol.%. The mixtures were stirred until the complete solubility of the dicarboxylic acid. For the sample containing sebacic acid, 10 mL of butanol were added to solubilize the dicarboxylic acid. The obtained mixtures were dried at 70 °C for 48 h. The obtained polymer films were heated from 70 to 120 °C with a heating rate of ≈1.5 °C min^{-1}. The samples were removed from the oven after 1 h of heating, resulting in LPVA-Seb for the sample containing sebacic acid, LPVA-Ad for the sample containing adipic acid and LPVA-Suc for the sample containing succinic acid.

Preparation of PVA TC-PNs: "Twin-chain" PVA polymer network gels were prepared following a procedure reported elsewhere,[23,31] where the PVA polymer with lower degree of hydrolysis (in the current work, LPVA modified with dicarboxylic acids) was originally used to induce the formation of a sponge-like disordered and interconnected porosity in the network of the PVA with similar molecular weight (HPVA). 10 m/v% solution of HPVA in pure water was mixed with a 10 m/v% solution containing the functionalized LPVA (LPVA-Seb, LPVA-Ad or LPVA-Suc) in order to achieve a HPVA to porogen ratio of 3 to 1. After 45 min of stirring at 70 °C the mixture was cast on plastic molds and stored at −20.0 °C for16 h. The resulting gels were thawed at room temperature, were swollen in pure water for 1 week, and were named PVA-Seb, PVA-Ad, and PVA-Suc according to the nomenclature given to the crosslinked LPVA porogens.

Labeling of H-PVA with FITC: H-PVA was chemically labeled with FITC, as reported in previous works.[23,27,31]

Cleaning Tests on Tartrazine-Dyed Cardboards: Cardboard sheets were soaked in demineralized water and then in a 2.5% w/w tartrazine aqueous solution for 1 min. Thus, they were air-dried. TC-PN gel sheets were gently dried on Whatman blotting paper and placed in contact with the dyed cardboard for 10 min. The gels cleaning efficacy was calculated, by using Image J software, on the greyscale image of the cleaned cardboard. The average, minimum and maximum values of pixels were calculated in 4 × 4 mm^2 squares, centered in the cleaned areas (black pixels intensity value = 0, white pixels intensity value = 255).

Cleaning Tests on Model Alkyd Surfaces: Cleaning tests were performed on an alkyd painted mockup mimicking modern/contemporary painting techniques, prepared using a commercial primed canvas, and oil (Windson&Newton) and alkyd colors (Ferrario). The mockup exhibits surface roughness with cavities and crests around 1–5 mm, similar to paint layers typical of modern art paintings (Jackson Pollock, Pablo Picasso, and others). The painted surface was soiled by brushing with an artificial soil mixture reported in the literature (Tate soil), comprising organic and inorganic particle dust.[24]

Prior to application, the TC-PN gel sheets were divided into 2 × 2 cm^2 sheets and loaded overnight with a tri-ammonium citrate (TAC) water solution (5% wt.). Afterward, the gel sheets were gently squeezed with blotting paper to remove water excess and laid in contact with the soiled mock-up surfaces. Overall, the procedure was performed for an application time of 3 min for each cleaning system, with no mechanical action.

Instruments, Cord Analysis, and Tortuosity: *Size Exclusion Chromatography (SEC)*: SEC measurements were performed utilizing a system composed of a Shodex ERC–3215α degasser connected with a Waters 1525 binary HPLC pump, a Waters 1500 series heater set at 50 °C, a Wyatt miniDAWN TREOS detector, a Wyatt Viscostar–II detector and a Wyatt OPTILAB T–rEX detector, a Shodex pre–column GPC KD–G 4A, and a Shodex column GPC KD–806 M employing a DMSO / DMF (70 / 30) mixture as eluent with a flow rate of 0.7 mL min^{-1}. A set of polyethylene oxide standards (PEO, 3 kg mol^{-1} < Mn <969 kg mol^{-1}) samples were purchased from PSS (PEOkit) and used for calibration. All data evaluation was performed according to standard procedures employing ASTRA software.

Confocal Laser Scanning Microscopy (CLSM): CLSM images were acquired by a Leica TCS SP8 confocal microscope (Leica Microsystems GmbH, Wetzlar, Germany), with a 63X/1.2 Zeiss water immersion objective. The 488 nm laser line (Ar laser) was used to excite both FITC and Rhodamine 110 chloride, i.e., the dye used to chemically label H-PVA in pre-gel solutions and the aqueous-soluble dye dissolved in the final gels, respectively. Fluorescence was collected with a photomultiplier tube (PMT) in the 498–540 nm range. 3-Dimensional confocal stacks of both pre-gel solutions and gels were acquired, containing 150–170 2D images.

Chord Analysis: 2D images extracted from gels confocal stacks were analyzed through the chord analysis distribution method.[38,39] A characteristic pore dimension, λ, was extracted. Chord analysis was performed with the MATLAB algorithm by M. Ryan MacIver adapted to read and analyze the Leica format (.lif) data from the confocal microscope.[44] About 80 images of each confocal stack were analyzed. Images were binarized at first, then a set of 10 000 randomly oriented lines was drawn on them. Chords, i.e., separated segments, are obtained each time a line crosses phase-boundaries. Chords of specific lengths are binned according to their occurrence to obtain the plot of their frequency, f(R), versus their dimension, R (μm). Data shown are the averages of trends extracted for each 2D image. The persistence length λ, describing the samples average pore size, is obtained from the slope of the exponential decay in the f(R) VS R semi-log graph:

$$f_{Pores}(R) \propto \exp\left(-\frac{R}{\lambda_{Pores}}\right) \quad (3)$$

with $1/\lambda$ the slope of the function in the semi-log graph. The minimum chord length considered was set to 2 pixels. Uncertainties on data were

obtained from the fitting procedure, implemented through the software Igor Pro 6.37.

Fluorescence Correlation Spectroscopy (FCS): FCS measurements were performed through the Leica CLSM apparatus used also for imaging, combined with the FCS modulus from PicoQuant (PicoQuant, Berlin, Germany). A Hybrid SMD detector was used to collect the fluorescence signal. Data fitting was performed assuming a three-dimensional Brownian diffusion of the fluorescent species through a 3D-ellipsoidal Gaussian volume. Such diffusion was assumed as the only contribution to the observed decay time. FCS curves were averaged (12–15 repetitions) and analyzed according to a single-component decay:

$$G(\tau) = \frac{1}{N}\left[\left(1+\frac{\tau}{\tau_D}\right)^{-1}\left(1+\frac{\tau}{S^2\tau_D}\right)^{-\frac{1}{2}}\right] \quad (4)$$

where N the average number of fluorescent species diffusing inside the confocal volume ($N = CV$, with $V = \pi^{3/2}\, w_0{}^3 S$ and C the concentration), τ_D the decay time and $S = z_0/w_0$ the ratio between the axial and the lateral dimensions of the confocal volume, determined through a calibration procedure (Alexa Fluor 568, 25 nM aqueous solution). The diffusion coefficient D is calculated as:

$$\tau_D = \frac{w_0{}^2}{4D} \quad (5)$$

Gels apparent tortuosity was determined considering the diffusion of Alexa Fluor 568 within TC-PN gels. The dye diffusion was measured after the gels contact with tartrazine-dyed cardboards (10 min contact). The diffusion coefficient of Alexa Fluor 568 in a 2.5% w/w tartrazine solution was used as comparison (free dye).

Effective Relative Diffusivity and Tortuosity: The apparent tortuosity of gels was calculated as the reciprocal of the effective relative diffusivity:[45,46]

$$\tau^2{}_{app} = \frac{\tau^2}{\epsilon} = \frac{D_{sol}}{D_{gel}} \quad (6)$$

where τ^2 is the tortuosity factor, τ the geometrical tortuosity and ϵ is the gels porosity. τ^2/ϵ was calculated for gels after the interaction with tartrazine-dyed cardboards (10 minutes interaction). The gels apparent tortuosity factor was calculated considering the diffusion coefficients of the dye Alexa Fluor 568 in a tartrazine aqueous solution (D_{Sol}) and inside the gels (D_{Gel}), respectively. D_{Sol} and D_{Gel} were obtained from FCS data fitting.

Small-Angle X-Ray scattering (SAXS): SAXS data were collected with a Xeuss 3.0 HR (Xenocs) instrument, with a GeniX 3D Cu High Flux Very Long Focus (HFVL) Complete x-ray generator equipped with a high brightness Cu X-ray tube (30 W/40 µm) and a FOX 3D single reflection multilayer optic. The scattered signals were collected with a Dectris Eiger 2R 1 M hybrid photon counting detector (pixel dimension of 75 × 75 µm2). After collection of 2D SAXS images, circular averaging was performed through the XSACT software, to plot data as Intensity versus Q (with Q the scattering vector, $Q = (4\pi/\lambda)\sin\theta$, and 2θ the scattering angle). Data were collected at two sample-to-detector distances: 450 and 1800 mm. The 2 data sets were corrected by subtracting the scattering intensities of water (normalizing for the time of measurement and the relative transmission factors) and the combined in a single curve trough the XSACT software. Glassy carbon was used to convert the intensity in absolute scale, considering the thickness of each sample.[47] The Q range of data collection was 0.007–0.54 $Å^{-1}$.

SAXS data fitting was performed through the software SASView [http://www.sasview.org/]. The scattered intensity, I(q), was assumed to be the sum of two contributions and a background:[48,49]

$$I(q) = I_L(0)\frac{1}{\left[1+\frac{D+1}{3}\left(q^2\xi^2\right)\right]^{D/2}} + I_G(0)\, exp\left(-\frac{q^2R^2}{3}\right) + Bkg \quad (7)$$

The Lorentzian term describes the scattering due to polymer chains in a liquid-like environment, while the Guinier term refers to the scattering of more dense objects. $I_L(0)$ and $I_G(0)$ define the relative weight of the two terms in the equation. D is the fractal dimension, ξ is the correlation length of polymer chains in liquid-like domains and R is the radius of gyration of gels solid-like junctions, i.e., polymer crystallites.

Acknowledgements

Massimo Bricchi (Regional Marketing Manager, Kuraray Europe GmbH) and Kuraray Europe are gratefully acknowledged for providing POVAL polymers. CSGI and the European Union (GREENART project, Horizon Europe research and innovation program under grant agreement no. 101060941) are gratefully acknowledged for financial support. Views and opinions expressed are, however, those of the author(s) only and do not necessarily reflect those of the European Union or the European Research Executive Agency (REA). Neither the European Union nor the granting authority can be held responsible for them. The publication was made by a researcher (RM) with a research contract co-funded by the European Union – PON Research and Innovation 2014–2020 in accordance with Article 24, paragraph 3a of Law No. 240 of December 30, 2010, as amended and Ministerial Decree No. 1062 of August 10, 2021 and by (DB) with a research contract funded by the European Union-PNRR NextGenerationEU in accordance with Article 24, paragraph 3a of Law No. 240 of December 30, 2010, as amended and Ministerial Decree No. 1365 of November 8, 2022.

Conflict of Interest

The authors declare no conflict of interest.

Data Availability Statement

The data that support the findings of this study are available from the corresponding author upon reasonable request.

Keywords

crosslinking, cultural heritage preservation, hydrogels, porogen, PVA polyvinyl alcohol, "twin-chain" gels

Received: March 11, 2024
Revised: March 25, 2024
Published online:

[1] D. Bandelli, R. Mastrangelo, G. Poggi, D. Chelazzi, P. Baglioni, *Chem. Sci.* **2024**, *15*, 2443.
[2] C. Howell, A. Grinthal, S. Sunny, M. Aizenberg, J. Aizenberg, *Adv. Mater.* **2018**, *30*, 1802724.
[3] A. Walther, *Adv. Mater.* **2020**, *32*, 1905111.
[4] M. Chaouat, C. L. Visage, W. E. Baille, B. Escoubet, F. Chaubet, M. A. Mateescu, D. Letourneur, *Adv. Funct. Mater.* **2008**, *18*, 2855.
[5] A. Jafari, S. Vahid Niknezhad, M. Kaviani, W. Saleh, N. Wong, P. P. Van Vliet, C. Moraes, A. Ajji, L. Kadem, N. Azarpira, G. Andelfinger, H. Savoji, *Adv. Funct. Mater.* **2024**, *34*, 2305188.
[6] K. Chen, Y. Xiong, D. Wang, Y. Pan, Z. Zhao, D. Wang, B. Z. Tang, *Adv. Funct. Mater.* **2024**, *34*, 2312883.
[7] H. Liu, S. Wei, H. Qiu, M. Si, G. Lin, Z. Lei, W. Lu, L. Zhou, T. Chen, *Adv. Funct. Mater.* **2022**, *32*, 2108830.
[8] A. B. Shodeinde, A. C. Murphy, H. F. Oldenkamp, A. S. Potdar, C. M. Ludolph, N. A. Peppas, *Adv. Funct. Mater.* **2020**, *30*, 1909556.

[9] H. Chen, X. Ren, G. Gao, *ACS Appl. Mater. Interfaces* **2019**, *11*, 28336.
[10] C. Shao, L. Meng, M. Wang, C. Cui, B. Wang, C.-R. Han, F. Xu, J. Yang, *ACS Appl. Mater. Interfaces* **2019**, *11*, 5885.
[11] G. Davidson-Rozenfeld, X. Chen, Y. Qin, Y. Ouyang, Y. S. Sohn, Z. Li, R. Nechushtai, I. Willner, *Adv. Funct. Mater.* **2024**, *34*, 2306586.
[12] X. Du, Y. Bi, P. He, C. Wang, W. Guo, *Adv. Funct. Mater.* **2020**, *30*, 2006305.
[13] B. G. Brunetti, G. Sgamellotti, A. J. Clark, *Acc. Chem. Res.* **2010**, *43*, 693.
[14] A. Sgamellotti, B. G. Brunetti, C. Miliani, A. Sgamellotti, B. G. Brunetti, C. Miliani, *Science and Art: The Painted Surface*, The Royal Society of Chemistry, Piccadilly, London **2014**.
[15] R. Mastrangelo, D. Chelazzi, P. Baglioni, *Nanoscale Horiz.* **2024**, *9*, 566.
[16] L. Baij, J. Hermans, B. Ormsby, P. Noble, P. Iedema, K. Keune, *Heritage Sci.* **2020**, *8*, 43.
[17] A. Casoli, Z. Di Diego, C. Isca, *Environ. Sci. Pollut. Res.* **2014**, *21*, 13252.
[18] A. Casini, D. Chelazzi, P. Baglioni, *Sci. China Technol. Sci.* **2023**, *66*, 2162.
[19] G. Poggi, H. D. Santan, J. Smets, D. Chelazzi, D. Noferini, M. L. Petruzzellis, L. Pensabene Buemi, E. Fratini, P. Baglioni, *J. Colloid Interface Sci.* **2023**, *638*, 363.
[20] G. Pizzorusso, E. Fratini, J. Eiblmeier, R. Giorgi, D. Chelazzi, A. Chevalier, P. Baglioni, *Langmuir* **2012**, *28*, 3952.
[21] J. A. L. Domingues, N. Bonelli, R. Giorgi, E. Fratini, F. Gorel, P. Baglioni, *Langmuir* **2013**, *29*, 2746.
[22] M. Baglioni, J. A. L. Domingues, E. Carretti, E. Fratini, D. Chelazzi, R. Giorgi, P. Baglioni, *ACS Appl. Mater. Interfaces* **2018**, *10*, 19162.
[23] R. Mastrangelo, D. Chelazzi, G. Poggi, E. Fratini, L. Pensabene Buemi, M. L. Petruzzellis, P. Baglioni, *Proc. Natl. Acad. Sci. USA* **2020**, *117*, 7011.
[24] V. Rosciardi, D. Chelazzi, P. Baglioni, *J. Colloid Interface Sci.* **2022**, *613*, 697.
[25] V. Rosciardi, P. Baglioni, *J. Colloid Interface Sci.* **2023**, *630*, 415.
[26] V. Rosciardi, D. Bandelli, G. Bassu, I. Casu, P. Baglioni, *J. Colloid Interface Sci.* **2024**, *657*, 788.
[27] R. Mastrangelo, C. Resta, E. Carretti, E. Fratini, P. Baglioni, *ACS Appl. Mater. Interfaces* **2023**, *15*, 46428.
[28] E. A. Podorozhko, G. R. Ul'yabaeva, N. R. Kil'deeva, V. E. Tikhonov, Y. A. Antonov, I. L. Zhuravleva, V. I. Lozinsky, *Colloid J.* **2016**, *78*, 90.
[29] V. I. Lozinsky, L. G. Damshkaln, M. G. Ezernitskaya, Y. K. Glotova, Y. A. Antonov, *Soft Matter* **2012**, *8*, 8493.
[30] B. M. Budhlall, K. Landfester, E. D. Sudol, V. L. Dimonie, A. Klein, M. S. El-Aasser, *Macromolecules* **2003**, *36*, 9477.
[31] D. Bandelli, A. Casini, T. Guaragnone, M. Baglioni, R. Mastrangelo, L. Pensabene Buemi, D. Chelazzi, P. Baglioni, *J. Colloid Interface Sci.* **2024**, *657*, 178.
[32] A. Lederer, J. Brandt, in DOI: B978-0-12-819768-4.00012-9 (Eds: M. I. Malik, J. Mays, M. R. Shah), Elsevier, Amsterdam, The Netherlands **2021**, pp. 61.
[33] D. M. Meunier, J. W. Lyons, J. J. Kiefer, Q. J. Niu, L. M. DeLong, Y. Li, P. S. Russo, R. Cueto, N. J. Edwin, K. J. Bouck, H. C. Silvis, C. J. Tucker, T. H. Kalantar, *Macromolecules* **2014**, *47*, 6715.
[34] J. E. Puskas, W. Burchard, A. J. Heidenreich, L. D. Santos, *J. Polym. Sci., Part A: Polym. Chem.* **2012**, *50*, 70.
[35] A. Monaco, B. Drain, C. R. Becer, *Polym. Chem.* **2021**, *12*, 5229.
[36] L. Pensabene Buemi, M. L. Petruzzellis, D. Chelazzi, M. Baglioni, R. Mastrangelo, R. Giorgi, P. Baglioni, *Heritage Sci.* **2020**, *8*, 77.
[37] M. Baglioni, R. Mastrangelo, P. Tempesti, T. Ogura, P. Baglioni, *Colloids Surf. A* **2023**, *660*, 130857.
[38] P. Levitz, D. Tchoubar, *J. de Phys. I* **1992**, *2*, 771.
[39] P. Levitz, *Cem. Concr. Res.* **2007**, *37*, 351.
[40] P. M. Costich, H. W. Osterhoudt, *J. Appl. Polym. Sci.* **1974**, *18*, 831.
[41] C. Mazzuca, L. Micheli, M. Carbone, F. Basoli, E. Cervelli, S. Iannuccelli, S. Sotgiu, A. Palleschi, *J. Colloid Interface Sci.* **2014**, *416*, 205.
[42] C. Mazzuca, L. Micheli, E. Cervelli, F. Basoli, C. Cencetti, T. Coviello, S. Iannuccelli, S. Sotgiu, A. Palleschi, *ACS Appl. Mater. Interfaces* **2014**, *6*, 16519.
[43] N. Bonelli, C. Montis, A. Mirabile, D. Berti, P. Baglioni, *Proc. Natl. Acad. Sci. USA* **2018**, *115*, 5932.
[44] M. R. MacIver, M. Pawlik, *Chem. Eng. Technol.* **2017**, *40*, 2305.
[45] J. Hurler, A. Engesland, B. Poorahmary Kermany, N. Škalko-Basnet, *J. Appl. Polym. Sci.* **2012**, *125*, 180.
[46] M. Huang, J. F. Kennedy, B. Li, X. Xu, B. J. Xie, *Carbohydr. Polym.* **2007**, *69*, 411.
[47] F. Zhang, J. Ilavsky, G. G. Long, J. P. G. Quintana, A. J. Allen, P. R. Jemian, *Metall. Mater. Trans. A* **2010**, *41*, 1151.
[48] S. Mallam, F. Horkay, A. M. Hecht, A. R. Rennie, E. Geissler, *Macromolecules* **1991**, *24*, 543.
[49] M. Shibayama, T. Tanaka, C. C. Han, *J. Chem. Phys.* **1992**, *97*, 6829.